

## AIR QUALITY IMPACTS OF THE OCTOBER 2003 SOUTHERN CALIFORNIA WILDFIRES

H. PHULERIA, P.M. FINE AND C. SIOUTAS

Department of Civil and Environmental Engineering, University of Southern California, 3620 S. Vermont Avenue, Los Angeles, CA 90089

Keywords: wildfires, PM, co-pollutants.

### INTRODUCTION

In Southern California, dry summers followed by hot and dry westerly wind conditions contribute to the region's autumn fire season. In late October of 2003, 13 large Southern California wildfires burned more than 750,000 acres of land, destroyed over 3,500 structures, and displaced approximately 100,000 people. The fire episode was declared the deadliest and most devastating in more than a decade, and local media advised individuals to stay indoors to avoid exposure to excessive levels of PM, CO, VOCs, and ozone caused by the wildfires. This study examines the actual impact of these wildfires on air quality in urban Los Angeles using "opportunistic" data from other air pollution studies being conducted at the time of the fires

### METHODS

As part of the routine sampling of an ongoing study associated with the University of Southern California (USC) Children's Health Study (CHS), supported by the South Coast Air Quality Management District and the California Air Resources Board, concentrations of carbon monoxide (CO), ozone (O<sub>3</sub>), nitrogen oxide (NO), nitrogen dioxide (NO<sub>2</sub>), particulate matter less than 10  $\mu$ m (PM<sub>10</sub>) and particle number (PN) are continuously measured in several locations in Southern California. Continuous data were collected concurrently throughout the calendar year 2003, and five sites within the LA Basin impacted by the wildfires were examined in this study: Long Beach, Glendora, Mira Loma, Upland and Riverside. In addition to the data collected at the CHS sites, semi-continuous PM<sub>2.5</sub> (fine) and ultrafine PM mass concentrations were measured at the Southern California Supersite located near downtown Los Angeles at the University of Southern California (USC). Two-hour PM mass concentration data was collected with a Beta Attenuation Monitor (BAM). Finally, in a concurrent but unrelated study, particle size distributions were measured indoors and outdoors of a two-bedroom apartment in the Westwood Village area near the University of California, Los Angeles. The residence is located about 100 m mostly downwind (east) of the I-405 freeway, a very busy traffic source. A Scanning Mobility Particle Sizer (SMPS 3936, TSI Inc., St. Paul, MN) was set up in a bedroom and sampled alternating indoor and outdoor size distributions on a 24-hr basis.

### RESULTS AND DISCUSSION

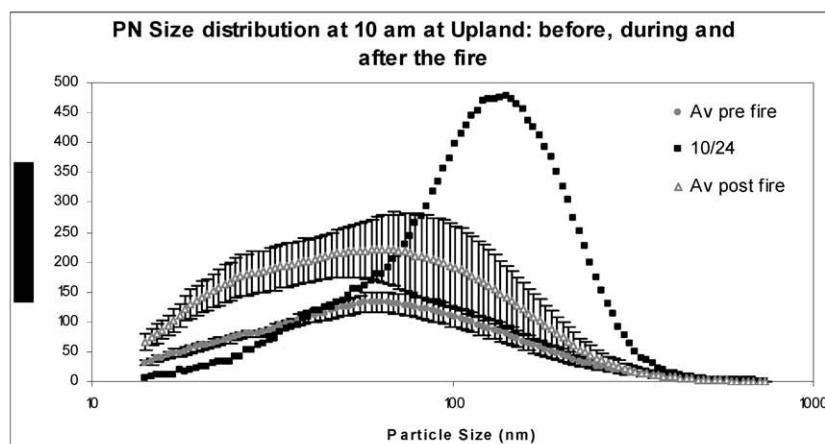
A summary of the average concentrations of the pollutants before, during and after the fire is given in Table 1. As surmised from the news reports and the data, the period of fire influence was from the 23<sup>rd</sup> to the 29<sup>th</sup> of October. The data summary in Table 1 indicates that with the exceptions of NO<sub>2</sub> and O<sub>3</sub>, the concentrations of almost any pollutant during the fire event were significantly higher (at the  $p=0.05$  level) than their respective values preceding the fire event. The rapid decline is associated with the wind reversal on the afternoon of the 29<sup>th</sup> when an on-shore wind pattern replaced the Santa Ana conditions, followed by rainfall on October 30 and 31.

**Table 1:** Average concentrations of pollutants with the standard deviation at the five CHS sites before, during and after the fire

	Average Concentration ( $\pm$ SD)					
	CO (ppm)	NO (ppb)	NO <sub>2</sub> (ppb)	O <sub>3</sub> (ppb)	PM <sub>10</sub> ( $\mu\text{g}/\text{m}^3$ )	PN (particles/cm <sup>3</sup> ) $\times 10^{-6}$
<b>Pre Fire</b>						
Glendora	8.9 $\pm$ 2.8	11.4 $\pm$ 15.5	37.0 $\pm$ 15.5	37.2 $\pm$ 21.3	12.4 $\pm$ 14.1	104.3 $\pm$ 54.8
Long Beach	6.4 $\pm$ 6.2	22.8 $\pm$ 48.5	47.2 $\pm$ 19.4	28.9 $\pm$ 17.7	33.1 $\pm$ 16.4	193.1 $\pm$ 124.4
Mira Loma	5.7 $\pm$ 4.2	44.9 $\pm$ 53.9	29.4 $\pm$ 14.3	25.4 $\pm$ 25.9	61.0 $\pm$ 35.1	161.9 $\pm$ 82.2
UC Riverside	7.7 $\pm$ 6.3	39.7 $\pm$ 29.1	32.8 $\pm$ 18.7	29.4 $\pm$ 29.3	47.2 $\pm$ 22.8	162.2 $\pm$ 121.2
Upland	9.6 $\pm$ 3.6	23.6 $\pm$ 28.4	44.3 $\pm$ 16.0	20.9 $\pm$ 23.0	38.6 $\pm$ 18.1	89.6 $\pm$ 36.6
<b>During Fire</b>						
Glendora	<b>11.2 <math>\pm</math> 5.0</b>	<b>24.5 <math>\pm</math> 29.7</b>	38.9 $\pm$ 28.1	43.6 $\pm$ 23.1	<b>26.7 <math>\pm</math> 24.6</b>	122.3 $\pm$ 62.2
Long Beach	<b>13.7 <math>\pm</math> 8.6</b>	<b>55.3 <math>\pm</math> 68.0</b>	55.9 $\pm$ 24.3	<b>14.8 <math>\pm</math> 15.6</b>	<b>93.0 <math>\pm</math> 91.6</b>	180.3 $\pm$ 85.1
Mira Loma	<b>11.8 <math>\pm</math> 8.2</b>	<b>105.0 <math>\pm</math> 84.8</b>	38.7 $\pm$ 26.2	<b>16.9 <math>\pm</math> 17.7</b>	<b>214.5 <math>\pm</math> 171.3</b>	<b>285.3 <math>\pm</math> 146.4</b>
UC Riverside	<b>11.9 <math>\pm</math> 6.5</b>	<b>45.6 <math>\pm</math> 35.5</b>	42.3 $\pm$ 21.8	<b>17.9 <math>\pm</math> 20.9</b>	<b>120.6 <math>\pm</math> 112.1</b>	<b>287.5 <math>\pm</math> 161.0</b>
Upland	<b>15.2 <math>\pm</math> 7.4</b>	<b>42.7 <math>\pm</math> 33.9</b>	47.1 $\pm$ 23.5	<b>15.0 <math>\pm</math> 16.0</b>	<b>164.8 <math>\pm</math> 137.5</b>	Data not available
<b>Post Fire</b>						
Glendora	5.0 $\pm$ 1.8	4.8 $\pm$ 4.9	17.2 $\pm$ 11.1	30.8 $\pm$ 10.5	17.9 $\pm$ 28.8	110.4 $\pm$ 62.5
Long Beach	8.4 $\pm$ 5.6	39.2 $\pm$ 49.2	32.1 $\pm$ 11.2	16.3 $\pm$ 11.7	21.3 $\pm$ 10.0	85.9 $\pm$ 96.6
Mira Loma	3.8 $\pm$ 3.2	56.8 $\pm$ 45.1	19.9 $\pm$ 11.2	18.8 $\pm$ 14.5	27.8 $\pm$ 16.1	238.5 $\pm$ 107.6
UC Riverside	5.5 $\pm$ 3.5	14.2 $\pm$ 25.2	19.7 $\pm$ 10.3	22.8 $\pm$ 15.4	17.5 $\pm$ 9.8	174.1 $\pm$ 110.2
Upland	5.8 $\pm$ 4.0	21.4 $\pm$ 25.2	22.6 $\pm$ 11.5	16.7 $\pm$ 12.7	19.3 $\pm$ 10.3	167.4 $\pm$ 85.9

Data in bold indicate statistically significant difference between the pre- and during fire concentrations at  $p=0.05$

Figure 1 shows the one-hour averaged particle size distribution at Upland, a site immediately downwind of the wildfire zone. The particle size distribution at 10 am. The SMPS scans were averaged for different days before and after the fire, and compared to the same hour during the influence of the fires. It can be seen that the size distribution corresponding to the periods of fire influence significantly differs from those without the fire influence. The mode in the number-based particle size distribution spans from 100 to 300 nm and is indicative of the wildfire smoke. More detailed data including penetration of outdoor PM indoors during the fire event will be presented



#### ACKNOWLEDGEMENTS

This work was supported by the California Air Resources Board and the South Coast Air Quality Management District through grants 53-4507-7822 and 53-4507-7823 to USC. Additional funding was provided by the Southern California Particle Center and Supersite (SCPCS), funded by the U.S. EPA (STAR award #R82735201).

## FINE STRUCTURE OF ELEMENTAL AND AEROSOL MASS SIZE DISTRIBUTIONS IN URBAN ENVIRONMENT

Imre SALMA<sup>1</sup>, Willy MAENHAUT<sup>2</sup>, Nico RAES<sup>2</sup>, Rita OCSKAY<sup>1</sup> and Gyula ZÁRAY<sup>1</sup>

<sup>1</sup> Eötvös University, Environmental Chemistry, H-1518 Budapest, P.O. Box 32, Hungary,  
E-mail: salma@para.chem.elte.hu

<sup>2</sup> Ghent University, Institute for Nuclear Sciences, Proeftuinstraat 86, B-9000 Gent, Belgium

### METHODS

Comprehensive aerosol characterisation was carried out in downtown Budapest, Hungary from 23 April through 5 May 2002. Several filter-based samplers and impactors were deployed, and two on-line instruments were used in parallel during the intensive field campaign. Among the samplers were a small deposit area low pressure impactor (SDI, Maenhaut *et al.*, 1996) and a micro-orifice uniform deposit impactor (MOUDI, Marple *et al.*, 1991). The former device operates at a flow rate of 11 l/min, has 12 impaction stages with the cut-off aerodynamic diameters between 8.5–0.045  $\mu\text{m}$ , and it collects samples on polycarbonate film. The latter impactor was used at a flow rate of 30 l/min, its 10 impaction stages have cut-off values in the range of 9.9–0.053  $\mu\text{m}$ , and the samples were collected on pre-baked aluminium foil. The impaction efficiency for each stage of both impactors was calibrated with monodisperse aerosol. The sample collection was performed separately for daylight periods and nights; altogether 23 samples and 6 field blanks were collected by each sampler. The SDI samples were analysed by particle-induced X-ray emission spectrometry in Ghent for 29 elements. The MOUDI samples were weighed under controlled conditions on a microbalance for particulate mass. The analytical data were inverted into smooth size distributions by the computer program Micron (Wolfenbarger & Seinfeld, 1990), and the inverted data were then fitted by lognormal distributions (Winklmayr *et al.*, 1990) so that the mode concentrations (Conc), geometric mean aerodynamic diameters (GMAD) and geometric standard deviations (GSD) for all contributing modes were obtained.

### RESULTS

The mean modal characteristics for selected elements and particulate matter (PM) are summarised in Table 1. It shows that very often, several modes appeared in the mass size distributions. The accumulation mode for elements having significant contribution from anthropogenic sources like S, K, Ni, Cu, Zn, Cl, Pb and Br, and PM consisted of two peaks: a condensation (GMAD around 0.3  $\mu\text{m}$ ) and a droplet (sub-) mode (GMAD around 0.7  $\mu\text{m}$ ) as observed already earlier for S/sulphate and nitrate. The mean relative abundances of the sub-modes varied from element to element; in general the droplet sub-mode had larger than or similar contribution to the condensation sub-mode. However, the droplet sub-mode could not be identified in all samples. For PM, the two sub-modes had approximately the same relative abundance; they each contained about 30% of the PM<sub>10</sub> mass. In the coarse size range, usually two modes were identified for typically soil-derived elements like Al, Si, Ca, Ti and Fe. The mode characterised by the larger GMAD (typically of about 4  $\mu\text{m}$ ) was always present; it accounted for about 97% of the PM<sub>10</sub> mass. The other coarse mode with the smaller GMAD (typically of 0.9  $\mu\text{m}$ ) contained about 4% of the elemental mass. The latter mode was not detected in some samples. In order to demonstrate the existence of the coarse modes, experimental data, inverted size distribution and fitted modes obtained for Fe over the daylight period of 1 May are displayed in Fig. 1 as an example. For the other elements, the two coarse modes were present only for K and Cl. The mean coarse GMADs for PM (2.7 and 8.6  $\mu\text{m}$ ) were found to be different from those for the elements. It is noted that the size distributions of organic matter and nitrate that make up about 30% and 5% of the aerosol mass in the PM<sub>10</sub>–2.0 size fraction, respectively (Maenhaut *et al.*, 2003) have not been dealt with so far.

Table 1. Geometric mean aerodynamic diameter (GMAD), number of occurrence (No.) and relative mode concentration (RMC) for condensation, droplet and coarse modes in 23 urban aerosol samples

Species	Condensation mode			Droplet mode			Coarse mode 1			Coarse mode 2		
	GMAD [ $\mu\text{m}$ ]	No.	RMC [%]	GMAD [ $\mu\text{m}$ ]	No.	RMC [%]	GMAD [ $\mu\text{m}$ ]	No.	RMC [%]	GMAD [ $\mu\text{m}$ ]	No.	RMC [%]
Al		0			0		0.94	11	4	4.50	23	98
Si		0			0		0.96	15	4	4.72	23	97
Ca		0			0		0.96	14	4	4.79	23	98
Ti		0			0		0.90	17	4	4.86	23	97
Fe		0			0		0.90	22	7	4.08	23	93
Mn	0.29	18	5	0.76	23	13		0		3.92	23	83
S	0.30	23	48	0.59	22	44		0		3.91	19	12
K	0.31	23	22	0.71	21	14	2.28	7	15	4.61	23	61
Ni	0.29	23	20	0.76	21	11		0		4.04	23	70
Cu	0.31	14	5	0.79	21	10		0		3.66	23	87
Zn	0.29	23	12	0.87	23	28		0		4.37	23	56
Na	0.34	23	16	0.79	17	27		0		3.34	23	60
Cl	0.39	21	10				1.16	18	14	4.58	23	79
Pb	0.26	23	28	0.68	23	41		0		3.31	23	31
Br	0.32	23	60	0.63	16	28		0		3.79	23	20
PM	0.27	23	31	0.65	11	32	2.68	22	23	8.64	23	31

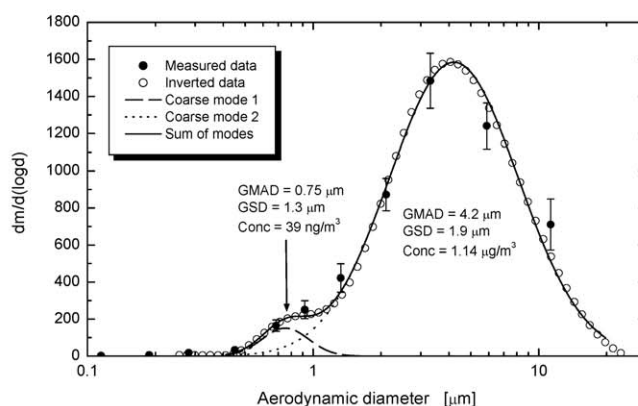


Fig. 1. Mass size distribution of Fe for daylight period on 1 May 2002 in downtown Budapest

## ACKNOWLEDGEMENTS

This work was supported by the Hungarian Scientific Research Fund (Contr. T043348) and by the Belgian Federal Science Policy Office (contract numbers EV/02/11A and BL/02/CR01).

## REFERENCES

- Maenhaut, W., Hillamo, R., Mäkelä, T., Jaffrezou, J.L., Bergin, M.H., Davidson, C.I. (1996). *Nucl. Instr. and Meth. B* **109/110**, 482.
- Maenhaut, W., Raes, N., Chi, X., Cafmeyer, J., Salma I. (2003). *J. Aerosol Sci.* **34** Suppl., S751.
- Marple, V.A., Rubow, K.L., Behm, S.M. (1991). *Aerosol Sci. Technol.* **14**, 434.
- Winklmayr, W., Wang, H.-C., John, W. (1990). *Aerosol Sci. Technol.* **13**, 322.
- Wolfenbarger, J.K., Seinfeld, J.H. (1990). *J. Aerosol Sci.* **21**, 227.

## **CORRELATION AND SPATIAL DISTRIBUTION OF PM<sub>10</sub> AND PM<sub>2.5</sub> CONCENTRATIONS BASED ON LONG-TERM SWISS MONITORING DATA**

R. GEHRIG<sup>1</sup> and B. BUCHMANN<sup>1</sup>

<sup>1</sup>Swiss Federal Laboratories for Materials Testing and Research, CH-8600 Dübendorf, Switzerland

**Keywords:** PM<sub>10</sub>/PM<sub>2.5</sub>, MEASUREMENTS, FINE PARTICLES.

### **INTRODUCTION**

Epidemiological studies have shown a significant impact of fine particles below 10 µm (PM<sub>10</sub>) on human health. Therefore, measurements of PM<sub>10</sub> have been performed within the Swiss National Monitoring Network (NABEL) already since 1997. Due to the increasing interest for the finer particles (PM<sub>2.5</sub>) the measurement programme of the network has been extended to include PM<sub>2.5</sub> measurements at 6 sites already in 1998. Since recently the EU-Commission expects member states to perform and report PM<sub>2.5</sub> measurements in addition to PM<sub>10</sub>. However, extended data sets of parallel PM<sub>2.5</sub> and PM<sub>10</sub> measurements are still lacking for Central Europe and even world-wide. Therefore, the Swiss data set forms a unique data basis for investigating the temporal and spatial behaviour of PM<sub>2.5</sub> compared to the well-known PM<sub>10</sub>. It includes meanwhile more than 5 years of parallel PM<sub>2.5</sub> and PM<sub>10</sub> data at various sites representing important exposition types of the population.

### **METHODS**

Collocated parallel measurements of PM<sub>2.5</sub> and PM<sub>10</sub> were conducted at 6 sites in Switzerland since January 1998 (Table 1) using High-Volume-Samplers Digitel DA 80 with subsequent gravimetric determination of the PM concentrations. The method is equivalent to the European reference method (EN12341). A more detailed discussion of the set-up and the findings of the parallel measurements can be found in Gehrig & Buchmann (2003).

### **RESULTS AND CONCLUSIONS**

Table 1 gives an overview of the long-term mean concentrations of PM<sub>10</sub> and PM<sub>2.5</sub> at the investigated sites for the 5 years from 1998-2002. The range of the long-term mean concentrations of PM<sub>2.5</sub> was between 8.1 µg/m<sup>3</sup> at Chaumont and 25.0 µg/m<sup>3</sup> in Lugano. For the sites within the Swiss plateau this range narrows from 15.3 µg/m<sup>3</sup> at the rural site of Payerne to 21.4 µg/m<sup>3</sup> at the directly traffic exposed site of Bern. The long-term averages of the PM<sub>2.5</sub>/PM<sub>10</sub> ratios of the daily values vary only from 0.74 to 0.76, with the exception of the traffic exposed site of Bern (0.60) indicating the influence of the local traffic as source of coarse particles. The correlation between the daily values of PM<sub>2.5</sub> and PM<sub>10</sub> at all sites is generally high ( $r^2 > 0.93$ ) with the exception of the sites Bern and Chaumont. The lower correlation at Bern reveals that the traffic induced coarse particles from abrasion and resuspension contained in PM<sub>10</sub> follow different temporal emission patterns than PM<sub>2.5</sub>, which is dominated by exhaust pipe emissions. This is plausible because mechanically produced particles, and in particular resuspension, depend not only on the vehicle frequency but also on the condition of the carriageway (e.g. clean/dirty, wet/dry). At the site of Chaumont the lower correlation can be explained with the generally lower concentrations and the correspondingly higher relative measurement uncertainties. Though the sites have quite different exposition characteristics, the correlation of the daily values of PM<sub>2.5</sub> and PM<sub>10</sub> between the different sites of the Swiss plateau is very high, indicating a dominant influence of regional meteorology over local events and sources. The left graph of Figure 1 shows the correlation for PM<sub>2.5</sub> between the sites Basel and Zürich as an example. Though the distance between these two sites is 72 km and they are separated by the 600-800m high Jura Mountains high correlation can be observed in particular in summer, but also during

wintertime. The right graph of Figure 1 shows a comparison of the two sites Payerne and Chaumont for PM<sub>2.5</sub>. The sites are located quite close together (distance 24 km) but on different altitudes. Chaumont is situated 650 m higher than Payerne. A high correlation can be observed during summertime, when the vertical mixing of the lower atmosphere is generally good and the absolute concentration level of the mountain site is only about 20% lower than at Payerne, which is situated within the Swiss basin in a rural environment. However, during wintertime, when the meteorology is characterised by frequent inversion, the observed PM<sub>2.5</sub> levels are largely decoupled. The correlation is very low and the absolute concentration level at the mountain site Chaumont reaches only about 20% of Payerne.

The findings imply that from the point of view of an efficient use of financial and personal resources, the number of collocated PM<sub>2.5</sub> measurements at PM<sub>10</sub> sites in a monitoring network can be kept quite limited. The saved resources could rather be used to investigate other particle related parameters providing substantial new information (e.g. on particle sources, formation and effects) like PM<sub>1</sub>, particle number concentrations, morphology or chemical composition.

Site	Site characteristics	PM <sub>10</sub> µg/m <sup>3</sup>	PM <sub>2.5</sub> µg/m <sup>3</sup>	PM <sub>2.5</sub> /PM <sub>10</sub>	r <sup>2</sup>
Basel	Suburban, quiet situation in a park	23.0	17.6	0.76	0.94
Bern	Urban, kerbside	36.1	21.4	0.60	0.86
Chaumont	Rural, elevated situation at 1140 m a.s.l.	11.3	8.1	0.75	0.84
Lugano	Urban, situated in a park, south of the Alps.	33.8	25.0	0.74	0.94
Payerne	Rural, 490 m a.s.l.	20.8	15.3	0.75	0.94
Zürich	Urban background, courtyard in the city centre.	24.4	18.2	0.75	0.93

Table 1. Investigated sites with long-term mean concentrations (1998-2002), mean daily PM<sub>2.5</sub>/PM<sub>10</sub> ratios and correlation coefficients of daily values

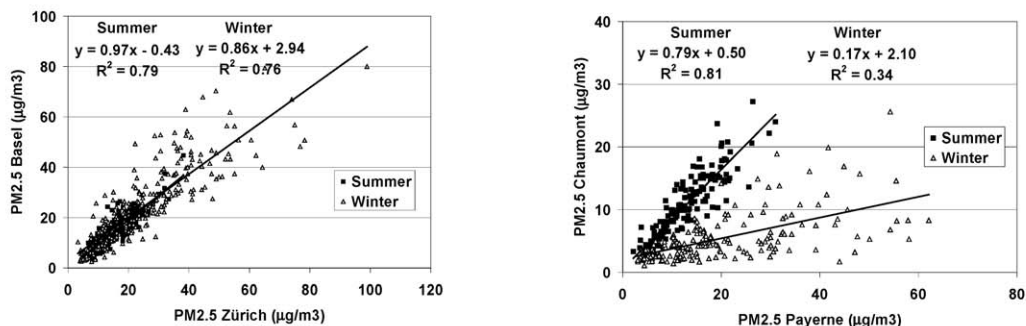


Figure 1. Scatterplot and linear regression of the daily values of PM<sub>2.5</sub> at Zürich and Basel (left) and at Payerne and Chaumont (right) during summer (June to August) and during winter (December to February)

#### ACKNOWLEDGEMENTS

This work was supported by Swiss Federal Agency for the Environment, Forests and Landscape.

#### REFERENCES

- Gehrig, R. & Buchmann, B. (2003). Characterising seasonal variations and spatial distribution of ambient PM<sub>10</sub> and PM<sub>2.5</sub> concentrations based on long-term Swiss monitoring data, *Atmospheric Environment* 37(19), 2571-2580.



## CONTRIBUTIONS OF LOCAL SOURCES TO THE DIURNAL VARIATION OF $PM_{10}$ MASS CONCENTRATIONS IN THREE DIFFERENT REGIONS IN GERMANY

U. QUASS, A. JOHN and T.A.J. KUHLBUSCH

IUTA e.V., Department Airborne Particles, Bliersheimer Str. 60, D-47229 Duisburg, Germany

Keywords: URBAN AEROSOL, ANTHROPOGENIC SOURCES, LIMIT VALUE, TRAFFIC.

### INTRODUCTION

The  $PM_{10}$  daily limit value set by a recent EU Directive is exceeded at several locations in Germany with much fewer locations exceeding the yearly limit value. Therefore the identification of relevant sources and source processes are necessary to develop effective action plans, as required by the EU legislation. These action plans shall ensure a lasting improvement of the air quality. Elevated aerosol mass concentrations in urban and agglomeration areas like e.g. the Rhine-Ruhr Area are partially due to sources with emissions varying regularly over the day and over the week. Sources influencing the diurnal variation of  $PM_{10}$  are especially traffic but also certain industrial processes. A previous study (Kuhlbusch *et al.*, 2000) revealed that diurnal variations of  $PM_{10}$  mass concentrations reflect the variations of local/regional sources within ca. 30 km distance. Therefore the analysis of diurnal concentration profiles enables a quantitative assessment of contributions of sources with regular source activities to the daily mean  $PM_{10}$  mass concentration.

### METHODS

Automatic (TEOM or Beta-absorption) as well as manual  $PM_{10}$  mass concentrations were taken from data sets generated within the framework of three projects carried out in Germany in 2002/2003 (Kuhlbusch *et al.*, 2003, John *et al.*, 2004, Quass *et al.*, 2004). A total of 14 different sites from 4 German states were analysed covering different station types (background, rural background, urban background, urban traffic and industrial).

Diurnal variations of  $PM_{10}$  mass concentrations were computed using  $\frac{1}{2}$ -hour or 1-hour mean values. The average and median values were calculated separately for each day (Sunday to Saturday) for four periods of 3 months each. Separation into four 3 months periods was done to account for effects due to varying meteorological conditions – in particular changing mixing heights – over the year.

To obtain quantitative estimates on  $PM_{10}$  contributions by sources with regular source activities, diurnal profiles were corrected with baseline profiles. The baseline profiles were constructed from a) the diurnal profiles obtained from a background site which is not influenced by local to regional sources and b) an ideal Sunday profile. The latter was derived from the true Sunday profile with the substitution of the hours from midnight to early morning by the corresponding values of the Monday profile. This correction was necessary as the early hours of Sunday frequently showed enhanced  $PM_{10}$  mass concentrations (c.f. Figure 1) probably due to Saturday night activities. The quantitative contribution of sources with regular diurnal source activities was now calculated by subtraction of both base lines from the calculated diurnal variations and averaging the remaining mass concentration. The ratio of these values to the total  $PM_{10}$  daily mean value yields the relative contribution of sources with regular diurnal source activities within an area of around 30 km.

### RESULTS AND CONCLUSIONS

Typical diurnal  $PM_{10}$  concentration profiles for the seven weekdays and for the “ideal Sunday” are displayed in Figure 1. They show an increase of  $PM_{10}$  mass concentrations in the morning hours and –slightly weaker – in the early afternoon. These peaks most probably relate to traffic intensity. Fig. 2 shows the relative  $PM_{10}$  mass contributions of local to regional sources over a week (after baseline corrections) for three

different station types in Rhineland-Palatinate. The local to regional source contribution to  $PM_{10}$  is significantly higher at the traffic and the industrial site compared to the urban background site. In addition, a general trend with increasing  $PM_{10}$  source contributions from Sunday to Friday followed by lower contributions on Saturday can be seen.

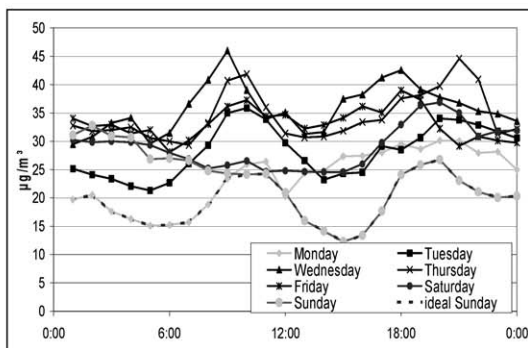


Figure 1. Diurnal variation of  $PM_{10}$  concentrations in Ludwigshafen, Germany (industrially influenced)

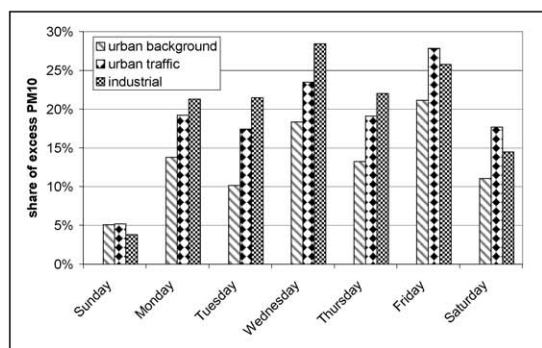


Figure 2. Relative contribution of local to regional sources with regular activities to  $PM_{10}$

#### Particular observations:

- The relative contribution at the industrial site is higher than at the traffic site on every workday except Friday and Saturday; this may indicate that part of excess  $PM_{10}$  is due to industrial processes which stop on early Friday whereas other activities (e.g. traffic) still remain on a considerable high level.
  - Particularly high  $PM_{10}$  mass concentrations on Saturdays in the 3<sup>rd</sup> and 4<sup>th</sup> quarter could be attributed to the beginning / end of summer holidays and to the shopping Saturdays preceding Christmas.
- $PM_{10}$  mass contributions of local/regional sources with regular source activities are given in table 1. These data show that the sources (ca. 30 km range) account for a relevant fraction of the  $PM_{10}$  mass concentration.

Results for further sites in Germany will be presented and discussed in detail also in view of the weekly trend in the exceedances of the daily limit values.

	Location	Urban background	Urban traffic	Industrial
RLP	(Kuhlbusch et al., 2003)	10 % – 21 %	17 % – 28 %	22 % – 28 %
NRW	(Quass et al., 2004)	14 % – 27 %	-	-

Table 1.  $PM_{10}$  mass contributions by local/regional sources with regular emission activities to total  $PM_{10}$  (Monday to Friday)

#### ACKNOWLEDGEMENTS

This work was supported by the Ministry of Environmental Protection of North Rhine-Westphalia (NRW), the Senate Department for Urban Development of Berlin and the State Environmental Protection Agency of Rhineland-Palatinate (RLP).

#### REFERENCES

- John, A.C., Kuhlbusch, T.A.J. (2004). *Ursachenanalyse von Feinstaub( $PM_{10}$ )-Immissionen in Berlin*, report to the Department for Urban Development of Berlin, IUTA-Bericht LP 09/2004.
- Kuhlbusch, T.A.J., John, A.C. (2000). *Korngrößenabhängige Untersuchungen von Schwebstaub und Inhaltsstoffen*, report to Ministry of Environmental Protection of North Rhine-Westphalia.
- Kuhlbusch, T.A.J., John, A.C., Romazanowa, O. Top, S., Weißenmayer, M. (2003). *Identifizierung von  $PM_{10}$ -Emissionsquellen im Rahmen der Maßnahmenplanung zur Reduktion der  $PM_{10}$ -Immissionsbelastung in Rheinland-Pfalz*, report to State Environmental Protection Agency of Rhineland-Palatinate, IUTA-Bericht LP 06/2003.
- Quass, U., Kuhlbusch, T.A.J., Schmidt, K.G., Fissan, H. (2004). *Quellenzuordnung für die Feinstaubfraktion*, report to Ministry of Environmental Protection of North Rhine-Westphalia, IUTA-Bericht LP 10/2004.



## AEROSOL CHARACTERISTICS FROM TAIWAN SUPERSITE DURING YELLOW DUST PERIODS

C.T. LEE<sup>1</sup>, M.T. TSUANG<sup>1</sup> and C.C. CHAN<sup>2</sup>

<sup>1</sup>Graduate Institute of Environmental Engineering, National Central University  
Jungli, Taoyuan, 320, Taiwan

<sup>2</sup>Institute of Occupational Medicine and Industrial Hygiene, National Taiwan University  
Taipei, 100, Taiwan

Keywords: AEROSOL SUPERSITE, ATMOSPHERIC AEROSOL, YELLOW DUST.

### INTRODUCTION

The sources regions of Asian yellow dust (YD) are distributed from deserts in North-western China, Inner Mongolia, and Mongolia. The YD drawn by a dust storm is frequently transported by Siberia High to China, Korea, and Japan, and in some occasions, to Taiwan (Lin, 2001), Hong Kong, and even to North America. As YD affecting Taiwan, it was observed to show an increase of wind speed accompanied with a low relative humidity as well as a rapid increase of  $PM_{10}$  concentration. This work reports aerosol characteristics from Taiwan aerosol Supersite (Supersite) in YD events in 2002.

### METHODS

The Supersite is located in a satellite city of Taipei metropolitan area. Detailed descriptions of instrument operation and maintenance are shown in Lee, *et al.* (2002). In 2002, Taiwan Environmental Protection Administration officially declared eight YD events affected Taiwan. The Supersite was able to observe aerosol properties from the second to the eighth YD events. In this work, an YD event is divided into before, during, and after periods for comparing aerosol characteristics. The during period of an YD event was observed to have a change in wind direction accompanied with an increase of wind speed and a dramatic increase of  $PM_{2.5-10}$  ( $PM_{10}-PM_{2.5}$ ). Herein, we designated 24 hours before the start of an YD event as the before period. For the after period of an YD event, we took the time when the wake of the passed continental high reached northern Taiwan. In this period, the airflow was from relatively clean Pacific Ocean; however, the aerosol was observed high especially for  $PM_{2.5}$ , probably resulted from poor ventilation of the atmosphere and the resurgence of local photochemical reactions.

### RESULTS AND DISCUSSION

Figure 1 shows the averages of  $PM_{2.5-10}$  and  $PM_{2.5}$  in the before, during, and after periods for the last 7 YD events in 2002. It demonstrates that  $PM_{2.5-10}$  is significant in the period during an YD event compared with the other two periods. Meanwhile,  $PM_{2.5}$  is noticed to be predominant in the after period. This phenomenon constitutes a typical YD aerosol observed in Taiwan.

Based on aerosol monitoring characteristics from Supersite, we found a difference in affecting time for each YD event. For instance, the affecting time was as long as 147 hours for the second YD event as compared with 7 hours for the last YD event. It is probably due to the differences in strength and the path of each continental high as well as the dusts picked up by the updraft wind. Interestingly, we found a strong correlation between the time of during period and the maximum  $PM_{10}$  or  $PM_{2.5-10}$  for each event. The  $R^2$  of linear regression models for the relationship between the time and the  $PM_{10, \max}$  or  $PM_{2.5-10, \max}$  are 0.98 and 0.96, respectively.

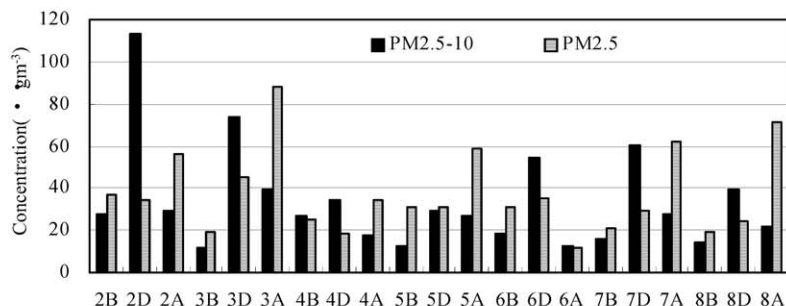


Fig. 1. Average concentration of  $PM_{2.5-10}$  and  $PM_{2.5}$  observed from each yellow-dust period in 2002 (2-8: number of yellow-dust event, B: before period, D: during period, A: after period).

As the affecting time was the longest in the second YD event, we report  $PM_{2.5}$ ,  $PM_{2.5}$  sulfate, and  $PM_{2.5}$  nitrate from this event in Figure 2.  $PM_{2.5}$  sulfate and  $PM_{2.5}$  nitrate are agreed well with  $PM_{2.5}$  especially for  $PM_{2.5}$  sulfate. By examining the back-trajectory of this YD event, we found the airflow above 1,000m was originated from Inner Mongolia, while the lower trajectory passed along the coastal area of East China. The peak concentration on March 10 was probably contributed from China's outflow plus the influence from the passed high-pressure wake, while that on March 12 was associated with another wake.

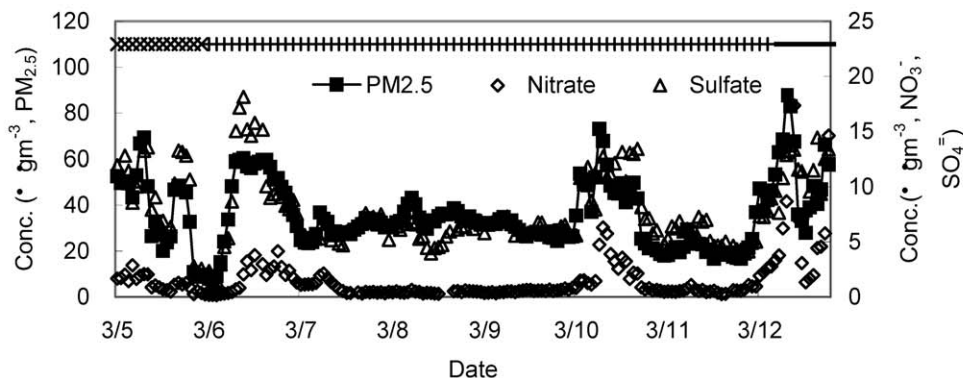


Fig. 2. Time variation of  $PM_{2.5}$ ,  $PM_{2.5}$  sulfate, and  $PM_{2.5}$  nitrate from the second YD event in 2002 (note : before, during, and after periods are marked in symbol  $\times$ ,  $+$ , and  $-$ ).

## CONCLUSIONS

For the YD events in 2002, we find a strong correlation between the time of event period and the maximum  $PM_{10}$  or  $PM_{2.5-10}$  for each event. The typical YD aerosol observed in Taiwan shows a significant  $PM_{2.5-10}$  during the event period and a rise of  $PM_{2.5}$  in the after period. The continuous monitoring from Supersite shows  $PM_{2.5}$ ,  $PM_{2.5}$  sulfate, and  $PM_{2.5}$  nitrate were associated with China's outflow and influenced by the wake of the passed continental high.

## REFERENCES

- Lee, C. T., Chou, C. C., & Chang, S. Y. (2002). *Supersite Operation and Maintenance in 2002*. Taiwan EPA, EPA-91-L105-02-206.
- Lin, T. H. (2001). *Long-range transport of yellowsand to Taiwan in Spring 2000: observed evidence and simulation*. *Atmos. Environ.*, 35, 5873-5882.

## TRAFFIC-RELATED SOURCE CONTRIBUTIONS TO PM<sub>10</sub> NEAR A HIGHWAY

Erik Swietlicki<sup>1</sup>, Torsten Nilsson<sup>1</sup>, Adam Kristensson<sup>1</sup>, Christer Johansson<sup>2</sup>, Gunnar Omstedt<sup>3</sup> and Lars Gidhagen<sup>3</sup>

<sup>1</sup> Division of Nuclear Physics, Lund University, P.O. Box 118, SE-211 00 Lund, Sweden.

<sup>2</sup> Institute of Applied Environmental Research, Air Laboratory, Stockholm University, Frescativägen 54, SE-10691 Stockholm, Sweden

<sup>3</sup> Swedish Meteorological and Hydrological Institute, SE-60176 Norrköping, Sweden

Keywords: PM<sub>10</sub>, traffic emissions, highway, road dust, studded tires.

### INTRODUCTION

Emissions of aerosol particles from traffic sources are relevant from both a health and a climate perspective. New EU legislation (Council Directive 1999/30/EC) puts high demands on society to reduce particle mass concentrations (PM<sub>10</sub>) in order to alleviate severe health effects to the population. It is therefore of considerable societal interest to determine the particle emissions caused by traffic, in order to provide the basis for efficient air quality management. Of particular importance for PM<sub>10</sub> concentration in urban environments are the non-tailpipe emissions associated with wear of the road surface and tires.

### METHOD

A 6-week monitoring campaign was undertaken close to the E4 highway 28 km north of Stockholm, Sweden during March-May 2003. At the chosen site, the 4-lane highway follows a straight line with open fields on both sides. Average traffic intensity during the campaign was 52 300 vehicles per day, with an average of 6% diesel fueled trucks and buses. Rush hour traffic intensity was around 5 000 vehicles per hour. More experimental details are found in Gidhagen *et al.* (2004), where inverse modelling was used to deduce tail-pipe emission factors of NO<sub>x</sub> and exhaust particles. Here, the focus is on the measurements of elemental composition of fine and coarse aerosol particle size fractions obtained from a PIXE (Particle Induced X-ray Emission) analysis of 12-h samples collected with an automatic filter sampler. Parallel measurements of PM<sub>10</sub> concentrations were performed with a TEOM.

### RESULTS

The PIXE elemental analysis produced a data set consisting of fine and coarse fraction 12-h averaged concentrations of Al, Si, S, Cl, K, Ca, Ti, Cr, Mn, Fe, Ni, Cu, Zn, As, Br, Sr and Pb, and fine fraction V, Se, Zr and Sn, as well as coarse fraction W. This data set was further analyzed with the multivariate source-receptor model PMF (Positive Matrix Factorization; Paatero, 1997). The purpose of the PMF analysis was to determine (i) the number of sources affecting the PM<sub>10</sub> concentrations close to the highway, (ii) to determine the nature (source mechanism) and composition of the sources, and finally (iii) to apportion the PM<sub>10</sub> concentrations to the various sources in a quantitative way.

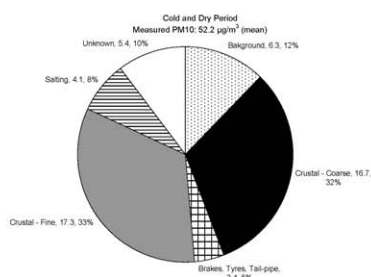


Figure 1. Source apportionment for the E4 highway site during a cold and dry period ( $\mu\text{g}\cdot\text{m}^{-3}$ , %).

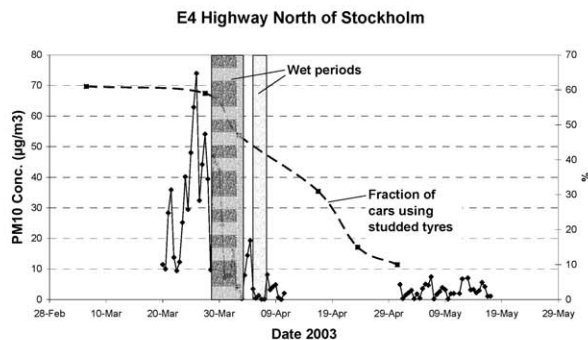


Figure 2. Time variation of the contribution of crustal material (fine and coarse) to PM10 concentrations, and the fraction of cars using studded tyres.

A PMF solution consisting of five sources was chosen. These sources were identified as, in order of importance for the PM10 concentrations: (1) a fine mode crustal source, (2) a coarse mode crustal source, (3) a long-range transported regional background source, (4) a source connected to salting of the highway, and finally (5) a source that is a mixture of wear of tires and brakes and probably also a contribution from tail-pipe emissions. The PMF 5-source model could account for 91% of the measured PM10 concentrations (6-week measured average:  $27.5 \mu\text{g}\cdot\text{m}^{-3}$ ) apportioned to the various sources according to: fine mode crustal (1)  $7.1 \mu\text{g}\cdot\text{m}^{-3}$ , coarse mode crustal (2)  $5.5 \mu\text{g}\cdot\text{m}^{-3}$ , background (3)  $5.3 \mu\text{g}\cdot\text{m}^{-3}$ , salting (4)  $4.4 \mu\text{g}\cdot\text{m}^{-3}$ , tires and tail-pipe (5)  $2.6 \mu\text{g}\cdot\text{m}^{-3}$ .

Figure 1 shows the contribution from the various sources during a cold and dry period. Crustal material in both the fine and coarse fraction originating from road wear constitute  $\sim 2/3$  ( $34 \mu\text{g}\cdot\text{m}^{-3}$ ) of the measured PM10 concentrations during this period. Figure 2 shows the effect of a wet road surface and the fraction of cars using studded tires on the concentration of the crustal (road wear) PM10 components. The conclusion is that restrictions on the use of studded tires would bring down PM10 levels considerably in near-traffic environments during winter and early spring. Other important traffic-related non tail-pipe sources to PM10 that could be identified were salting of the streets, and material from brakes and tires. Inverse modelling similar to the methodology in Gidhagen *et al.* (2004) will be used to deduce the source strengths of the traffic-related sources, and compare with model estimates.

#### ACKNOWLEDGEMENTS

This work was supported by the Swedish National Road and Traffic Administration (Vägverket) and the Stockholm County Council (Landstinget).

#### REFERENCES

- L. Gidhagen, C. Johansson, G. Omstedt, J. Langner and G. Olivares. Model simulations of NOx and ultrafine particles close to a Swedish highway, 2004, Submitted to *Env. Sci and Techn.*
- Paatero, P., Least squares formulation of robust non-negative factor analysis, 1997, *Chemom. Intell. Lab. Syst.* **37**, 23-35.